HOKKAIDO UNIVERSITY

Title	Nearly Temperature-Independent Saturation Drain Current in a Multi-Mesa-Channel AlGaN/GaN High-Electron-Mobility Transistor
Author(s)	Tamura, Takahiro; Kotani, Junji; Kasai, Seiya; Hashizume, Tamotsu
Citation	Applied Physics Express, 1(2), 023001 https://doi.org/10.1143/APEX.1.023001
Issue Date	2008-02-25
Doc URL	http://hdl.handle.net/2115/33900
Rights	Copyright © 2008 The Japan Society of Applied Physics
Type	article (author version)
File Information	APEX-tamura.pdf

Instructions for use

Hokkaido University Collection of Scholarly and Academic Papers : HUSCAP

Applied Physics Express Vol.1, Art.No. 023001, 2008

Nearly Temperature-Independent Saturation Drain Current in a Multi-Mesa-Channel AlGaN/GaN High-Electron-Mobility Transistor

Takahiro Tamura*, Junji Kotani, Seiya Kasai, and Tamotsu Hashizume†

Research Center for Integrated Quantum Electronics and Graduate School of Information Science and Technology, Hokkaido University, N13, W8, Kita-ku, Sapporo 060-8628, Japan

We fabricated a multi-mesa-channel (MMC) structure by forming a periodic trench just under a gate electrode to improve the uniformity of effective electric field in the channel in an AlGaN/GaN high electron mobility transistor (HEMT). A unique performance, i.e., a nearly temperature-independent saturation drain current, was observed in the MMC device in a wide temperature range. A 2-dimensional potential calculation indicates that the mesa-side gate effectively modulates the potential, resulting in a field surrounding 2-dimensional electron gas. Such a surrounding-field effect and a relatively lower source access resistance may be related to a unique current behavior in the MMC HEMT.

AlGaN/GaN high electron mobility transistors (HEMTs) have extensively been studied as devices operating under high-speed, high-power, and high-temperature conditions. A high cutoff frequency of 181 GHz has been obtained for a device with a gate length of 30 nm.[1] Dora *et al.*[2] reported a high breakdown voltage of 1900 V in a device using field-plate technology. However, these values are still lower than those predicted by the material parameters. One of the reasons for this is considered to be non-uniform distribution of the electric field in the channel[3, 4] and in the source access region.[5] In this case, such a field can enhance the breakdown process, and impede the effective acceleration of electrons in the channel.

We propose and characterize a multi-mesa-channel (MMC) AlGaN/GaN HEMT in this paper that can improve the uniformity of the effective electric field in the channel and gate controllability. A schematic illustration of the MMC HEMT is shown in **Fig. 1**. By forming a periodic trench, the MMC HEMT has parallel mesa-shaped channels with 2-dimensional electron gas (2DEG) surrounded by the gate electrode.

We used an $Al_{0.27}Ga_{0.73}N$/GaN heterostructure grown by metal organic chemical vapor deposition on a (0001) sapphire substrate in this study. The residual donor density of the undoped GaN layer (1 μm) was 1 x 10^{15} cm^{-3}. The AlGaN barrier consisted of undoped/Si-doped/undoped layers with a total thickness of 25 nm. The sheet carrier density and mobility of 2DEG at room temperature (RT) were 1.1 x 10^{13} cm^{-2} and 980 cm^2/Vs, respectively. First, the SiO_2 mask pattern was formed on the AlGaN/GaN structure by using electron beam lithography and wet etching. Then, we carried out reactive ion-beam etching of the patterned sample to form a periodic trench, assisted by electron-cyclotron-resonance plasma (ECR-RIBE) using a gas mixture of $CH_4/H_2/Ar/N_2$.[6] After the dry etching, the SiO_2 mask pattern was removed. A scanning electron microscopy (SEM) observation was used to confirm that the angle of the mesa-side facet was 62°,[7] as indicated in Fig. 1. The etching depth, *d*, was set to 50 nm to completely eliminate 2DEG in the trench region and to minimize plasma damage. To obtain the drain and source electrodes, a Ti/Al/Ti/Au multilayer was deposited and annealed at 800 °C for 1 min. Then, the Ni/Au gate electrode was deposited on the

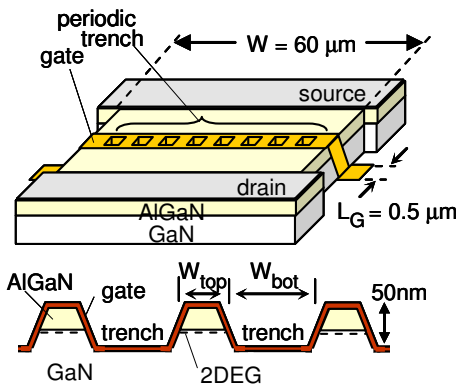

Fig. 1 Schematic illustration of MMC AlGaN/GaN HEMT

* E-mail address: tamura@rciqe.hokudai.ac.jp
† E-mail address: hashi@rciqe.hokudai.ac.jp

periodic-trench region. For comparison, we also fabricated a conventional planar-type HEMT without a trench. All the devices fabricated have a gate length, L_G, of 0.5 μm, a gate width, W, of 60 μm, and a gate-drain spacing of 1 μm. No passivation was carried out on their surfaces.

Figure 2 shows the drain current-voltage (I_{DS}-V_{DS}) characteristics of a conventional and the MMC HEMTs measured at RT. The MMC HEMT has a mesa-top width, W_{top}, of 60 nm and a trench-bottom width, W_{bot}, of 340 nm, resulting in 150 periods of mesa channels within the gate width, W, of 60 μm. Thus, the effective gate width, i.e., the sum of W_{top}, was 9 μm for the MMC structure. As shown in Fig. 2(b), the MMC HEMT demonstrated good *I-V* behavior with complete pinch-off behavior. We used an effective gate width of 9 μm, and expected the magnitude of the drain current to be only 15 % that of the planar device whose gate width was 60 μm. However, the MMC HEMT produced a drain current that was more than twice the expected value. The gate leakage current normalized by the effective gate width was almost the same between two devices, indicating that the leakage current through the mesa-gate area in the MMC HEMT is negligible compared with the top-gate.

The transfer characteristics of the planar and the MMC HEMTs, measured in the temperature range from 120 to 500 K, are shown in **Fig. 3**. For the conventional HEMT, the saturation drain current decreased as the temperature increased, as shown in Fig. 3(a). The transconductance, g_m, also decreased at high temperatures. These results are in agreement with the reports from other groups.[8-10] Surprisingly, on the other hand, the saturation drain current was almost independent of the temperature for the MMC HEMT, as shown in Fig. 3(b), which is extremely unique. Since neither HEMT had a temperature dependence of the threshold voltage V_{th}, respectively, we expected that the 2DEG concentration was almost constant within the temperature range measured.[11, 12] However, the V_{th} value in the MMC HEMT was 1.6 V shallower than that of the planar HEMT, as shown in Fig. 3.

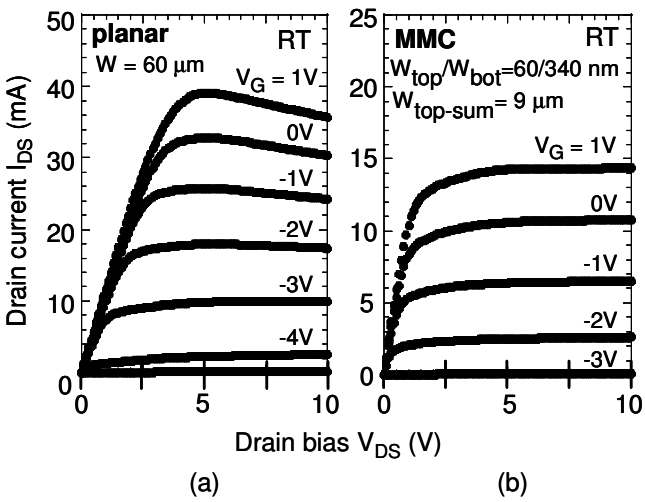

Fig. 2 I_{DS}-V_{DS} characteristics of (a) planar and (b) MMC HEMTs measured at RT

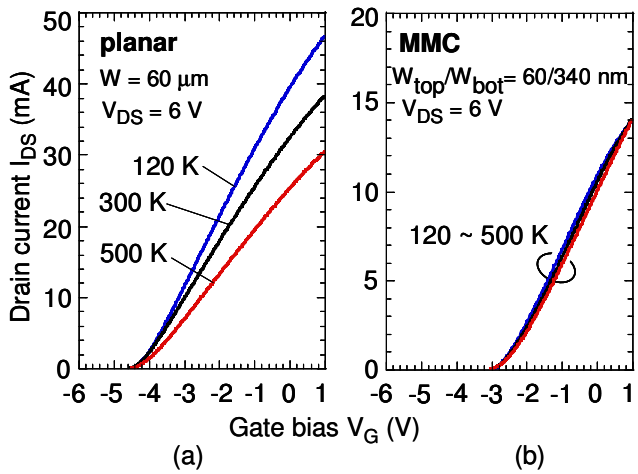

Fig. 3 Temperature dependence of transfer characteristics for (a) planar and (b) MMC HEMTs

To investigate the gate controllability in the MMC structure, the 2D potential distribution at the mesa cross-section was calculated for the structures with W_{top} = 200 and 60 nm. The gate bias was set to -2.5 V near the threshold voltage and the drain bias was 0 V. We used a Schottky barrier height (ϕ_B) of 1.4 eV in the calculation.[13] The results are shown in **Figs. 4**(a) and 4(b). For both structures, the side mesa-gates have lateral field effect on the edges of 2DEG. With decreasing the width of the top gate, the potential modulation through the undoped GaN layer becomes remarkable, resulting in a field surrounding 2DEG, as shown in Fig. 4(b). Figure 4(c) shows the 1D potential profiles along the depth direction at the center of the gate with W_{top} = 60 nm. Compared to the planar structure, the pulling-up of potential appears near 2DEG, causing the shallower V_{th} for the MMC HEMT.

We investigated the temperature dependence of the I_{DS}-V_{DS} characteristics at a fixed gate voltage to try to gain insight into the mechanism for the nearly temperature-independent saturation drain current in the MMC HEMT. As shown in **Fig. 5**, as the temperature increased, the current slope was reduced in the linear region for both the planar and

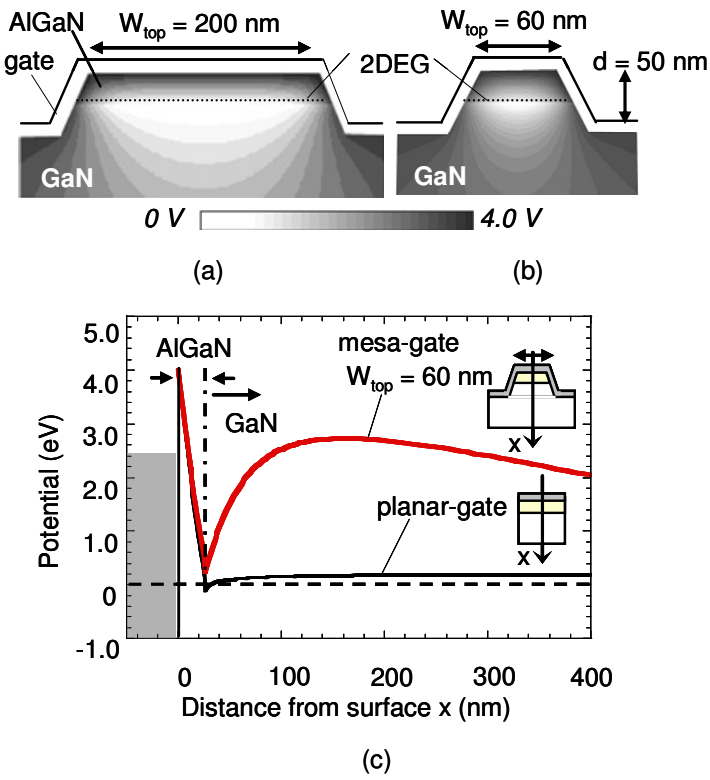

Fig. 4 2D-potential distributions of the MMC structures with W_{top} = 200 (a) and 60 nm (b). The gate and drain biases were –2.5 and 0 V, respectively. (c) 1D-potential distributions along depth direction for planar and MMC structures

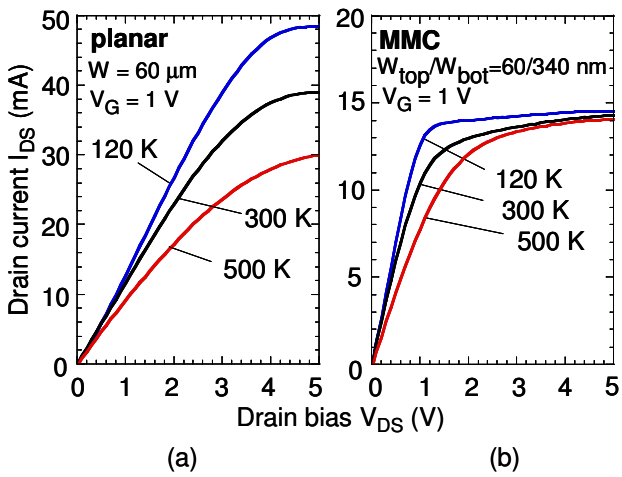

Fig. 5 Temperature dependence of I_{DS}-V_{DS} characteristics at V_G = 1 V for (a) planar and (b) MMC HEMTs

the MMC HEMTs. This mainly arises from the temperature dependence of mobility.[11, 12] For the conventional planar HEMT, the saturation drain current decreased with increasing temperature. Akita *et al.*[14] pointed out that the operation of the planar HEMTs in a current saturation region is in an intermediate state between mobility-dominant and peak-velocity-dominant transports, mainly due to an insufficient strength of the field in the channel (less than 50 kV/cm in their device). Even in our case, a mobility-dependent velocity reduction may cause the decrease in saturation current and g_m at high temperatures. In fact, the drift velocity for conventional AlGaN/GaN HEMTs has been reported as 1.0 ~ 1.8 x 10^7 cm/s,[15, 16] which is still smaller than the theoretically predicted peak value of 2.5 ~ 3.0 x 10^7 cm/s.[17, 18] Under a relatively low field condition, the scattering mechanisms by ionized impurity and polar-optical phonon are dominant, because the field-accelerated electron energy is low. As known, such scattering mechanisms have strong temperature dependence, resulting in the temperature-dependent saturation current observed in a conventional planar HEMT.

On the other hand, in the MMC HEMTs, the temperature dependence of the saturation drain current was weak, which is completely different from that of a conventional HEMT. In the MMC HEMT, it is expected that the surrounding-gate field improves the uniformity of the electric field in each mesa channel.[19, 20] Under uniform and high field conditions, electrons in the channel have higher energy. Then, acoustic phonon and inter-valley phonon processes are dominant in the scattering mechanism, and they have weak lattice temperature dependence.[21] In fact, the calculations using the Monte Carlo method [14, 21] predicted the weak temperature dependence of the drift velocity at higher electric fields (> 100 kV/cm). This may lead to the nearly temperature independent saturation drain current observed in the MMC HEMT. Another possibility is a relatively lower source access resistance for the individual mesa channels. This can improve the current drivability (g_m) in each mesa channel, being accompanied by the enhancement of the drift velocity. In this case, electrons in the channel can gain higher energy, thereby contributing to weak temperature dependence of the saturation current. In fact, Palacios *et al.* reported the influence of the dynamic source access resistance on the transconductance and drift velocity.[22] Since a single-channel mesa-gate device showed a similar temperature dependence of saturation current to the planar device (not shown here), the effect of source access region may be related to characteristic feature of saturation drain current in the MMC HEMT.

Although further investigation is needed for better understanding the transport mechanism, the unique characteristics observed in the MMC HEMT can help to open up a new application field in power electronics, because no temperature-compensation component or circuit is necessary for the MMC HEMT.

In summary, we proposed and characterized MMC AlGaN/GaN HEMTs. They exhibited a shallower threshold voltage than that of a conventional planar device. In addition, a nearly temperature-independent saturation drain current was observed in a wide temperature range from 120 to 500 K. The 2-dimensional potential calculation indicated that the mesa-side gate effectively modulates the potential, in addition to the mesa-top gate, resulting in a field surrounding 2DEG. Such a surrounding-field effect and a relatively lower source access resistance may be related to a unique temperature dependence of saturation drain current in the MMC HEMT.

References

1) M. Higashiwaki, T. Mimura, and T. Matsui: Jpn. J. Appl. Phys. **45** (2006) 1111.
2) Y. Dora, A. Chakraborty, L. McCarthy, S. Keller, S. P. DenBaars, and U. K. Mishra: IEEE Electron Device Lett. **27** (2006) 713.
3) M. Singh, Y.-R. Wu, and J. Singh: IEEE Trans. Electron Devices **52** (2005) 311.
4) Y. Aoi, Y. Ohno, S. Kishimoto, K. Maezawa, and T. Mizutani: Jpn. J. Appl. Phys. **45** (2006) 3368.
5) T. Palacios, L. Shen, S. Keller, A. Chakraborty, S. Heikman, S. P. DenBaars, U. K. Mishra, J. Liberis, O. Kiprijanovic, and A. Matulionis: Appl. Phys. Lett. **89** (2006) 073508.
6) Z. Jin, T. Hashizume, and H. Hasegawa: Appl. Surf. Sci. **190** (2002) 361.
7) T. Sato, T. Oikawa, H. Hasegawa, and T. Hashizume: J. Vac. Sci. Technol. B **24** (2006) 2087.
8) N. Maeda, T. Saitoh, K. Tsubaki, T. Nishida, and N. Kobayashi: Jpn. J. Appl. Phys. **38** (1999) 987.
9) M. Akita, S. Kishimoto, and T. Mizutani: IEEE Electron Device Lett. **22** (2001) 376.
10) C. Lu, X. Xie, X. Zhu, D. Wang, A. M. Khan, I. Diagne, and S. N. Mohammad: J. Appl. Phys. **100** (2006) 113729.
11) P. B. Shah, D. D. Smith, T. E. Griffin, K. A. Jones, and S. T. Sheppard: IEEE Trans. Electron Devices **47** (2000) 308.
12) S. B. Lisesivdin, S. Acar, M. Kasap, S. Ozcelik, S. Gokden, and E. Ozbay: Semicond. Sci. Technol. **22** (2007) 543.
13) J. Kotani, M. Kaneko, H. Hasegawa, and T. Hashizume: J. Vac. Sci. Technol. B **24** (2006) 2148.
14) M. Akita, K. Kishimoto, and T. Mizutani: Phys. Status. Solidi. **188** (2001) 207.
15) B. E. Foutz, S. K. O'Leary, M. S. Shur, and L. F. Eastman: J. Appl. Phys. **85** (1999) 7727.
16) K. Shiojima, T. Makimura, T. Suemitsu, and N. Shigekawa: Jpn. J. Appl. Phys. **44** (2005) 8435.
17) T.-H. Yu and K. F. Brennan: J. Appl. Phys. **91** (2002) 3730.
18) J. M. Barker, D. K. Ferry, S. M. Goodnick, D. D. Koleske, A. Allerman, and R. J. Shul: J. Vac. Sci. Technol. B **22** (2004) 2045.
19) J. P. Colinge: Solid-State Electron. **48** (2004) 897.
20) Y.–K. Choi, D. Ha, T.–J. King and J. Bokor: Jpn. J. Appl. Phys. **42** (2003) 2073.
21) A. F. M. Anwar, S. Wu, and R. T. Webster: IEEE Trans. Electron Devices **48** (2001) 567.
22) T. Palacios, S. Rajan, A. Chakraborty, S. Heikman, S. Keller, S. P. DenBaars, and U. K. Mishra: IEEE Trans. Electron Device **52** (2005) 2117.